Supporting Information

Water-chain mediated proton conductivity in mechanically flexible redox-active organic single crystals

Munshi Sahid Hossain[†a], Meena Ghosh[†b], Amit Mondal[a], Ajmal P[b], Monochura Saha[a], Chilla Malla Reddy*[a], Sreekumar Kurungot*[b] and Subhajit Bandyopadhyay*[a]

(a) Department of Chemical Sciences, Indian Institute of Science Education and Research (IISER) Kolkata, Mohanpur, Nadia, West Bengal 741246, India. E-mail: sb1@iiserkol.ac.in, cmreddy@iiserkol.ac.in

(b) Physical and Materials Chemistry Division, CSIR-National Chemical Laboratory, Pune, 411008 Maharashtra, India. E-mail: k.sreekumar@ncl.res.in

CONTENTS

General methods:

All reagents and solvents for synthesis were purchased commercially and used without further purification. Dichloromethane (DCM) was pre-dried over calcium hydride (CaH_2) and then distilled. Column chromatography was performed on Merck silica gel (100 – 200 mesh). Thin layer chromatographies (TLCs) were carried out with E. Merck silica gel 60-F254 plates. Yields are indicated to the chromatographically and spectroscopically pure compounds, except as otherwise indicated.

Physical measurements:

Nuclear Magnetic Resonance Spectroscopy: The ^{1}H NMR spectra were recorded on 400 MHz JEOL or 500 MHz Bruker spectrometer instruments. Similarly, ^{13}C NMR experiments were performed with 100 MHz Jeol and 125 MHz Bruker instruments using either residual solvent signals as an internal reference or from internal tetramethylsilane on the δ scale. The chemical shifts (δ) were reported in ppm and coupling constants (*J*) in Hz. The following abbreviations were used: m (multiplet), s (singlet), d (doublet), t (triplet), dd (doublet of doublet). The solvents used for the spectroscopy experiments were of the spectroscopic grades and were free from any fluorescent impurities.

High-Resolution Mass Spectrometry and Infrared Spectroscopy: HRMS data were obtained from an Acquity ultraperformance Bruker MaXis Impact liquid chromatography instrument by positive mode electrospray ionization (Q-TOF). FT-IR spectroscopy in the solid-state was performed with a Perkin Elmer Spectrum RX1 spectrophotometer using KBr disk method.

All data were processed either by Origin 8.0 or Origin 18 program. ChemBio Draw 15 Ultra software was used for drawing structures and processing figures.

Single Crystal X-Ray Diffraction: SCXRD data for Azo-DPA crystal was collected at 100 K on a SuperNova, Eos diffractometer using monochromatic Mo-Kα radiation (λ = 0.71073 Å) having a 300 μm beam size. Using Olex2, (1.2.9 version) (*1*) the structure was solved with the SHELXT structure solution program using intrinsic phasing algorithm and refined with the SHELXL refinement package using Least Squares minimization (*2*,*3*). Displacement parameters of all non-hydrogen atoms were refined anisotropically. All the crystal packing diagrams were prepared using Mercury (3.10.1 version).

Powder X-ray Diffraction: The PXRD patterns were collected at ambient conditions on a Rigaku SmartLab with a Cu-Kα radiation (1.540 Å). The tube voltage and amperage were set at 40 kV and 50 mA respectively. Sample was scanned between 5 and 50° 2θ with a step size of 0.02°. The instrument was previously calibrated using a silicon standard. The PXRD patterns of experimental and simulated (from experimental crystal structure) are given in Figure S8.

DSC and TGA analysis: Differential Scanning Calorimetry (DSC) experiments were conducted on a MettlerToledo DSI1 STARe instrument on accurately weighed samples (6.6 mg) placed in hermetically

sealed aluminium crucibles (40 µL) upon scanning in the range of 30 °C to 400 °C at a heating rate of 5 °C/min under a dry nitrogen atmosphere (flow rate 80 mL/min).

Thermogravimetric Analysis (TGA) was performed on a Mettler-Toledo TGA/SDTA 851e instrument. Approximately 10 mg of the sample was added to an aluminum crucible and heated from 30 to 400 °C at a rate of 5 °C/min (see Fig. S10).

Synthetic procedure:

Synthesis of azobenzene-4,4′-dicarboxylic acid 3

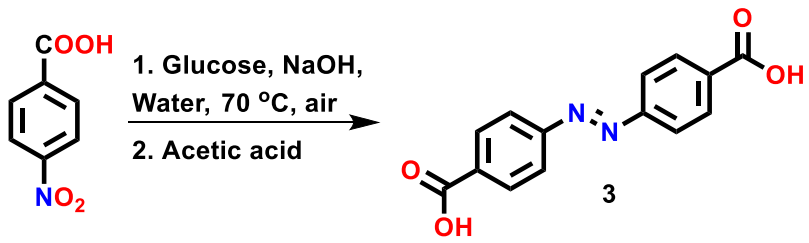

Azobenzene-4, 4'-dicarboxylic acid was synthesized according to the literature procedure (*4*). ^{1}H NMR (400 MHz, DMSO-d_6): δ 8.16 (d, J = 8.5 Hz, 4H), 8.0 (d, J = 8.5 Hz, 4H). ^{13}C{^{1}H} NMR (100 MHz, DMSO-d_6): δ 166.60, 154.13, 133.38, 130.68, 122.81. Given value is matching with the reported value.

Synthesis of (*E*)-4, 4'-(diazene-1,2-diyl)bis(N,N-bis(pyridin-2-ylmethyl)benzamide) 1

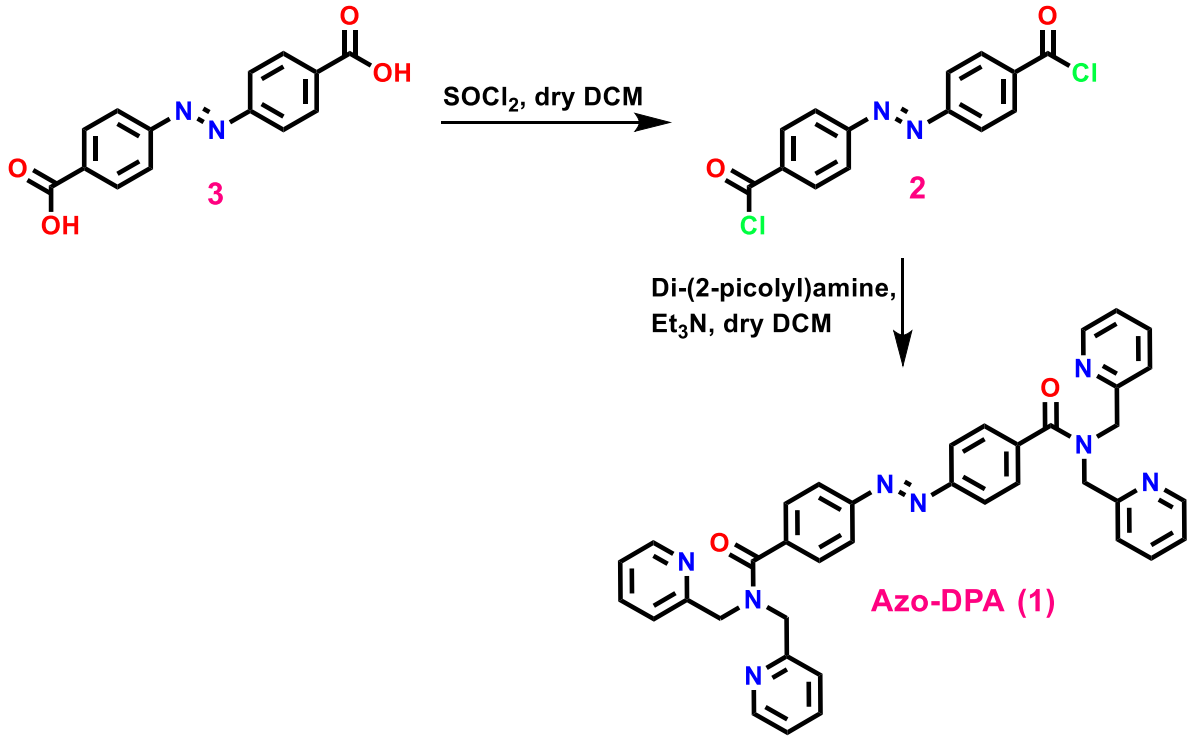

To the solution of azobenzene-4, 4'-dicarboxylic acid **3** (200 mg, 0.74 mmol) in dry DCM (10 mL), thionyl chloride (550 µL, 7.4 mmol) was added dropwise under the inert condition at 0 ^{O}C and the mixture was stirred for 12 h at room temperature, yielding a light pink solution. Excess thionyl chloride was removed by distillation and 4,4-bis(chlorocarbonyl)azobenzene **2** as a light pink solid (220 mg, crude) was obtained. The crude product was subsequently used without further purification.

To the solution of 4,4-bis(chlorocarbonyl)azobenzene **2** (220 mg, 0.716 mmol) in dry DCM (10 mL), triethylamine (500 µL, slight excess) and di-(2-picolyl) amine (313 µL, 2.2 mmol) were added and the reaction mixture was stirred for 6 h at room temperature. After completion of the reaction, DCM was evaporated under reduced pressure and the reaction mixture was extracted with ethyl acetate, dried over anhydrous Na_2SO_4 and concentrated under reduced pressure. The crude product was purified by column chromatography over silica gel (Eluent: 10% MeOH in ethyl acetate) to furnish the desired compound **1** (red crystalline solid, 270 mg, 59%); ^{1}H NMR (400 MHz, $CDCl_3$): δ 8.56 (m, 4H), 7.87 (d, J = 8.4 Hz, 4H), 7.72 (d, J = 8.4 Hz, 4H), 7.66 (m, 4H), 7.44 (d, J = 7.6 Hz, 2H), 7.19 (m, 6H), 4.89 (s, 4H), 4.70 (s, 4H); ^{13}C{^{1}H} NMR (100 MHz, $CDCl_3$): δ 171.9, 157.0, 156.3, 153.0, 150.0, 149.4, 138.6, 136.9, 128.1, 123.1, 122.8, 122.7, 122.5, 121.6, 54.4, 50.6; IR: v/cm^{-1} 3008, 2936, 1636, 1590, 1438, 1308, 1256, 1096, 998, 854, 754; (HRMS) m/z: $[M + H]^+$ Calcd for $C_{38}H_{32}N_8O_2H$, 633.2721; Found, 633.2719.

Characterizations

NMR spectroscopy:

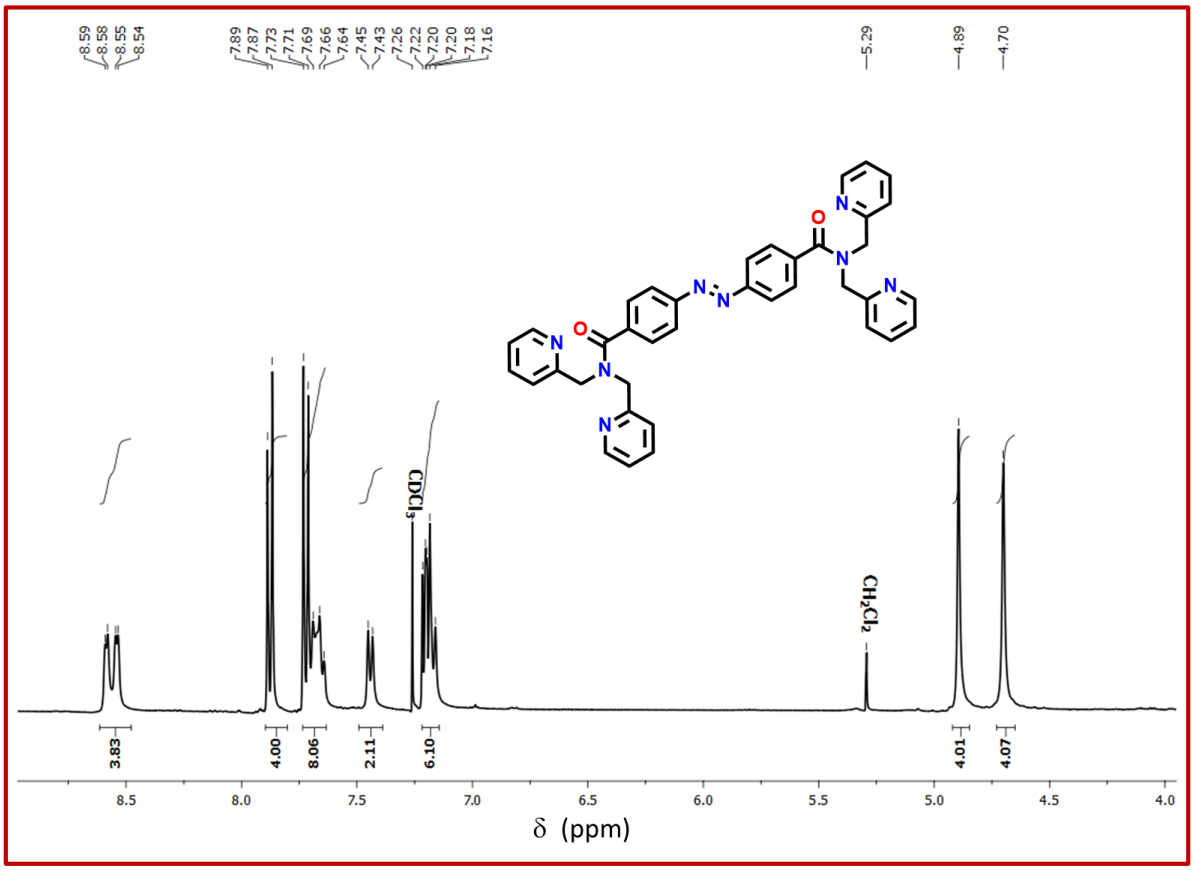

Figure S1: ^{1}H NMR (400 MHz) spectrum of Azo-DPA **1**.

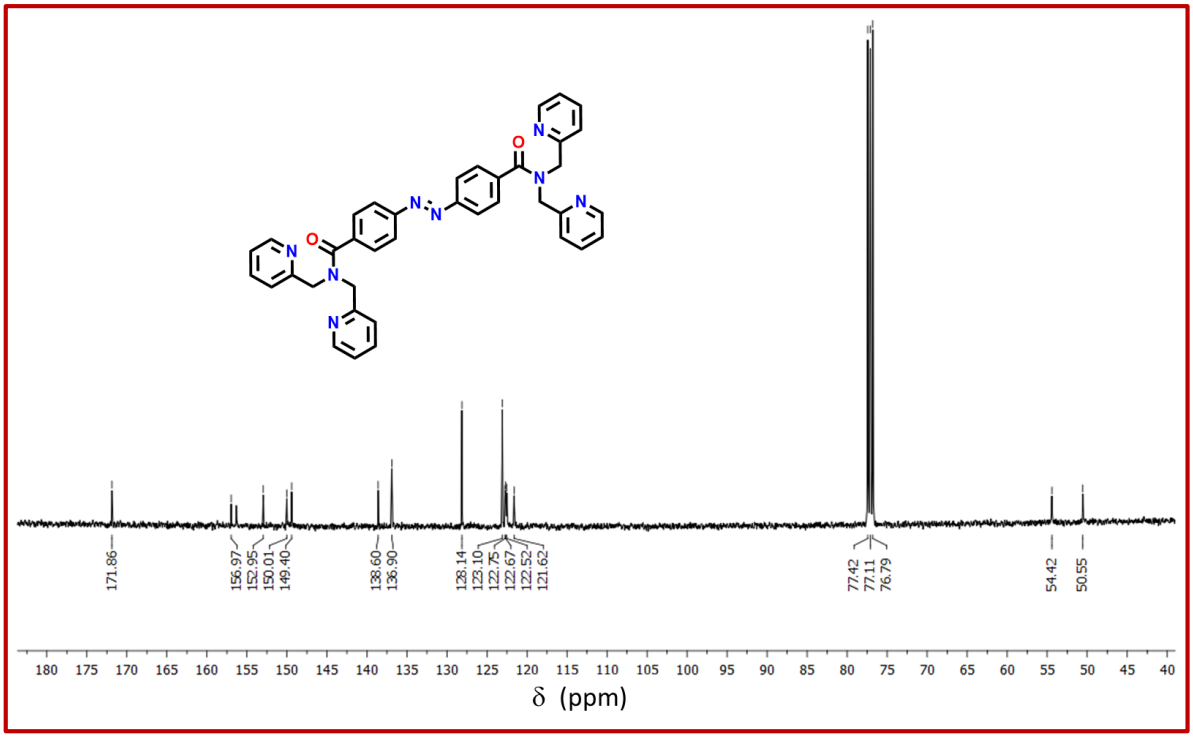

Figure S2: $^{13}C\{^{1}H\}$ NMR (100 MHz) spectrum of Azo-DPA **1**.

Mass spectrometry:

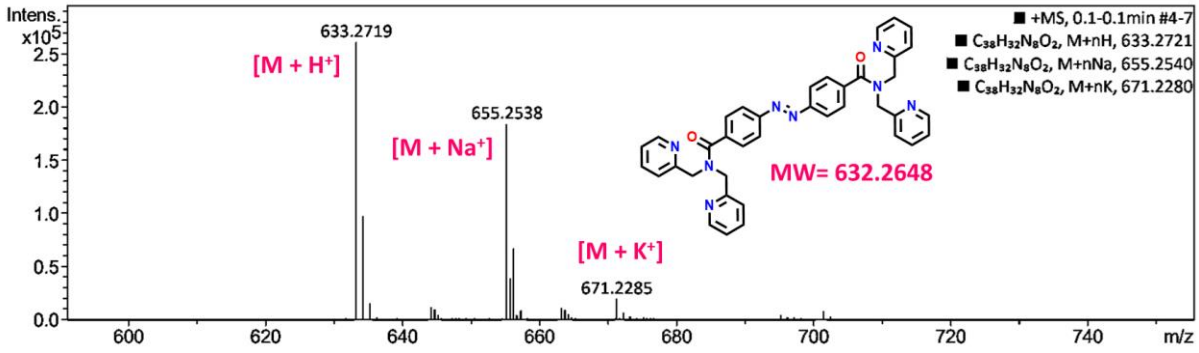

Figure S3: High-resolution mass spectrometry of Azo-DPA **1**.

Crystallization method:

After characterizing the compounds by NMR spectroscopy and mass spectrometry, as-synthesized Azo-DPA **1** (100 mg) was added to 10 mL of methanol in a nicely cleaned, dust-free conical flask to get a reddish solution. The solution was kept for 10-12 days to obtain reddish needle-shaped single crystals of **1**.

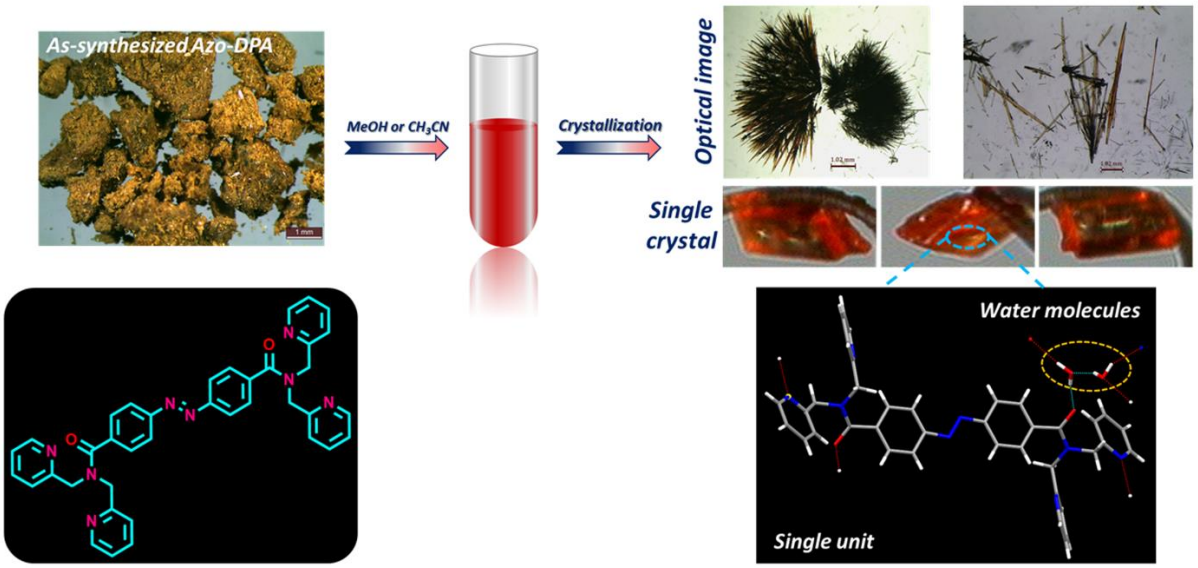

Figure S4: Schematic representation of crystallization process. Crystal structure displayed the presence of water molecules.

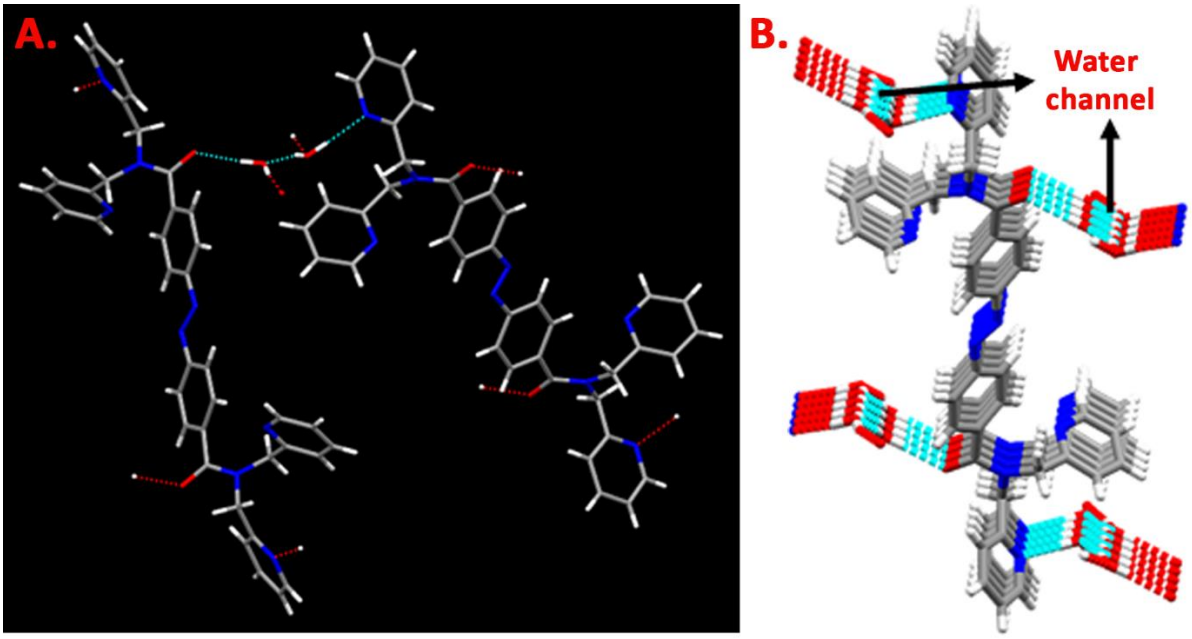

Figure S5: (A) Crystal structure showed that two Azo-DPA units are connected by two water molecules. (B) Oriental growth of the crystal exhibited the presence of water channels.

Crystallographic details:

Table S1: Crystallographic parameters of Azo-DPA crystal

Temperature (K)	100
Formula	$C_{19}H_{20}N_4O_3$
Formula Weight	352.39
Crystal System	Monoclinic
Space group	$P2_1/c$
a(Å)	17.3845(4)
b(Å)	5.02190(10)
c (Å)	20.0170(5)
V(Å^3)	1703.80(7)
$\alpha(^o)$	90
$\beta(^o)$	102.847(3)
$\gamma(^o)$	90
Z	4
D_c (g cm^{-3})	1.374
μ (mm^{-1})	0.096
θ range (°)	4.174 – 52.738
Reflections collected	16124
Unique reflections	3444
R_{int}	0.0278
GoF (obs/all)	1.053

R_F^{obs} ($I > 2\sigma(I)$)	0.04
wR_F^{all}	0.088
$\Delta\rho_{min}/\Delta\rho_{max}$ (eÅ^{-3})	0.27/-0.21
CCDC No.	2214530

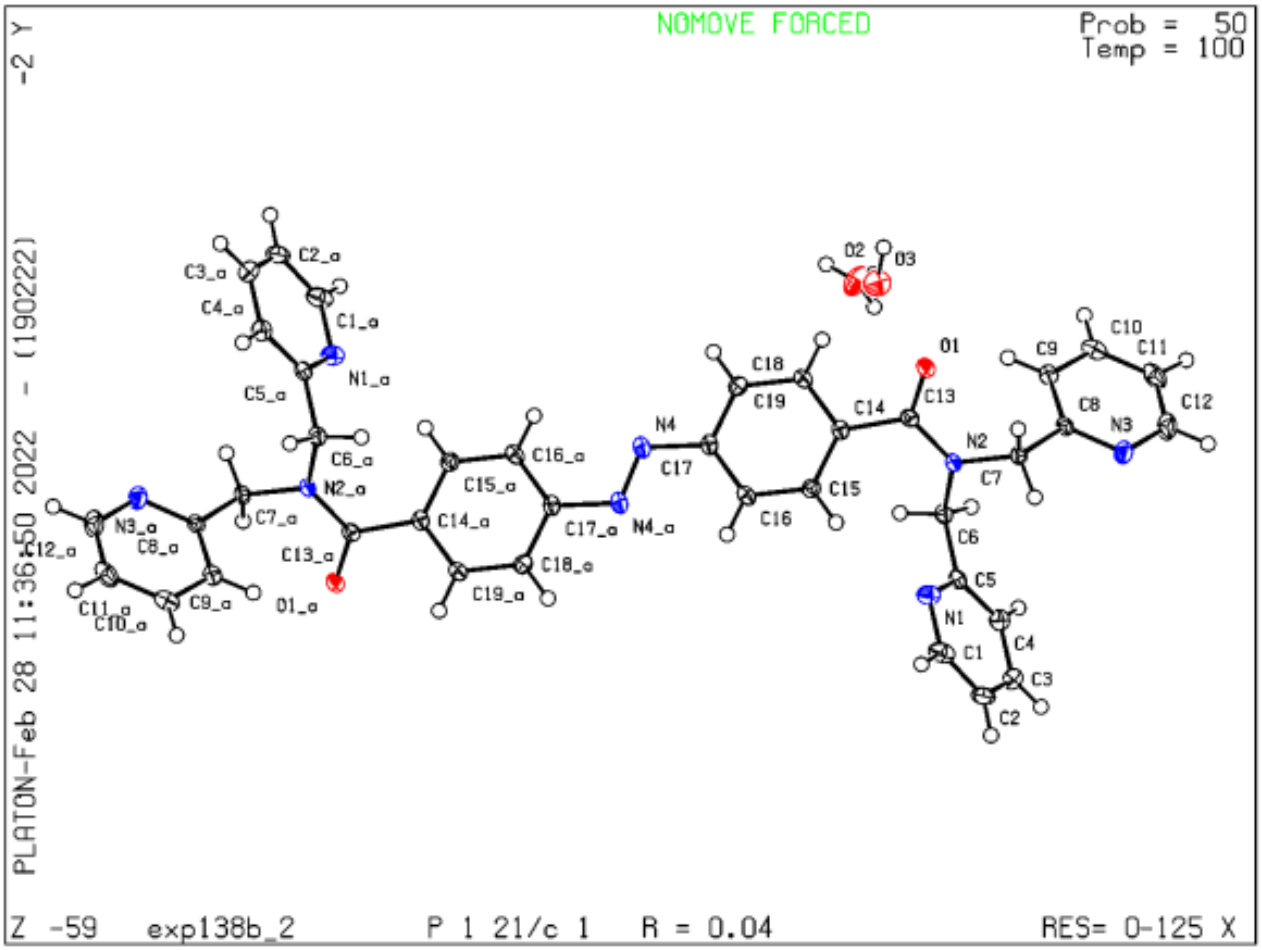

Figure S6: ORTEP diagram (with 50% thermal ellipsoid probability) of Azo-DPA **1.**

Infrared spectroscopy:

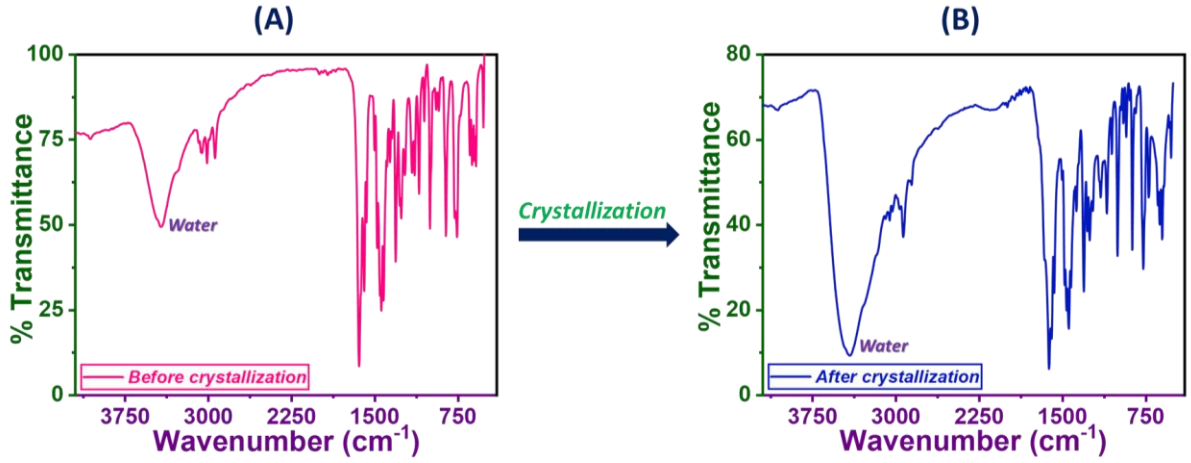

Figure S7: Infrared spectroscopy (A) As-synthesized Azo-DPA (small band at 3422 cm^{-1} for water) and (B) crystallized Azo-DPA (relatively large band at 3410 cm^{-1} for water molecules due to the presence of water channels).

Powder X-ray diffraction:

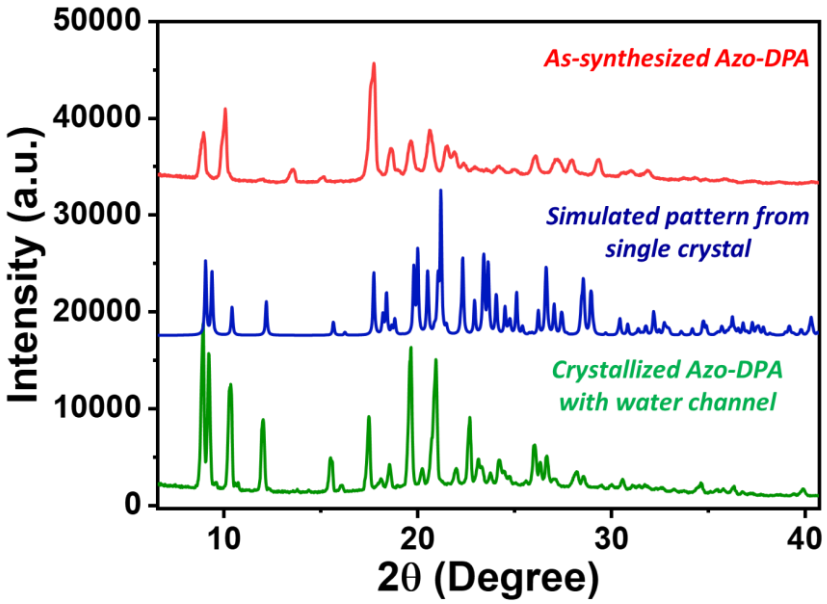

Figure S8: Powder X-ray diffraction of as-synthesized Azo-DPA (top), crystallized Azo-DPA (bottom), and simulated data from single-crystal (middle) where PXRD pattern of crystallized Azo-DPA is exactly similar to that of simulated pattern from single crystal which exhibits bulk phase purity and the presence of water channel in the bulk phase.

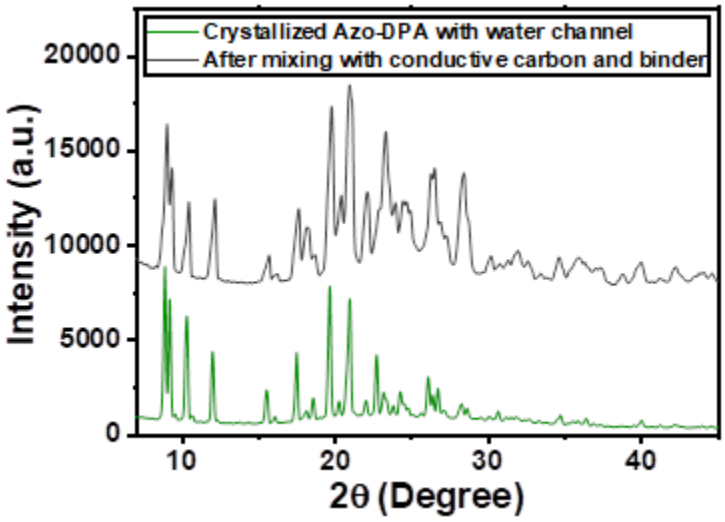

Figure S9: Powder X-ray diffraction pattern of the crystallized Azo-DPA (bottom) is matching with the slurry (a blend of crystallized Azo-DPA, binder, and conductive carbon, top) which shows that crystallized Azo-DPA retains its phase even in the blend.

Thermogravimetric Analysis (TGA) analysis and Differential Scanning Calorimetry (DSC) analysis:

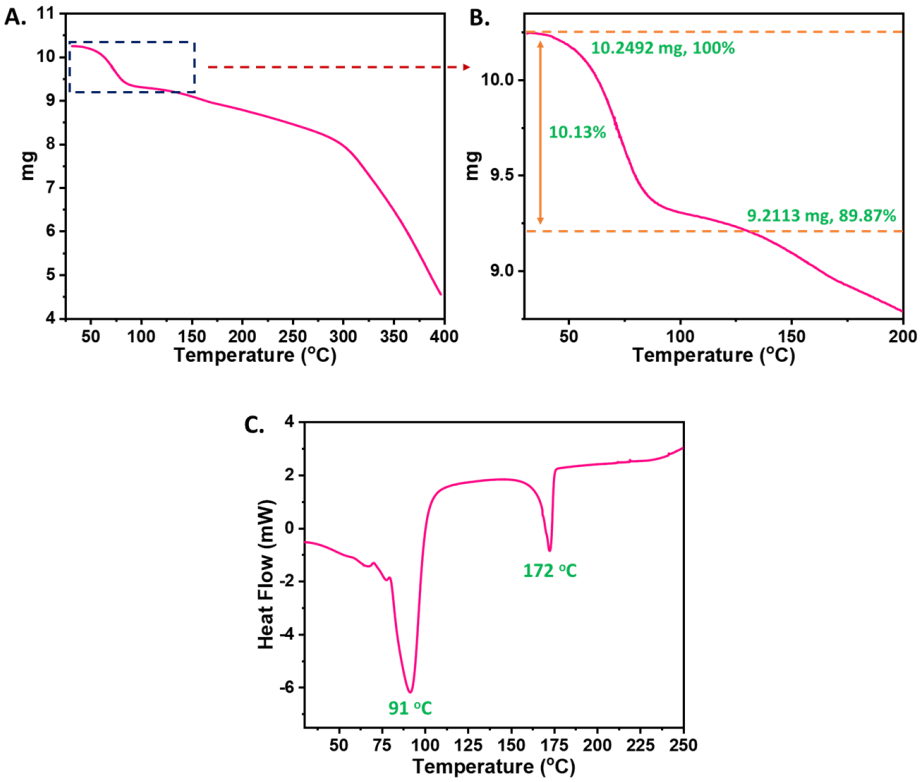

Figure S10. Thermal analysis of the crystallized Azo-DPA (A) TGA plot showing the decomposition of the sample after 300 °C; (B) Zoomed version of TGA (30 °C to 200 °C) displaying the water loss (1.03 mg) before 100 °C which is exactly matching with the calculated weight of water present within the sample; (C) DSC data exhibiting water loss around 90 °C, much before melting point (172 °C).

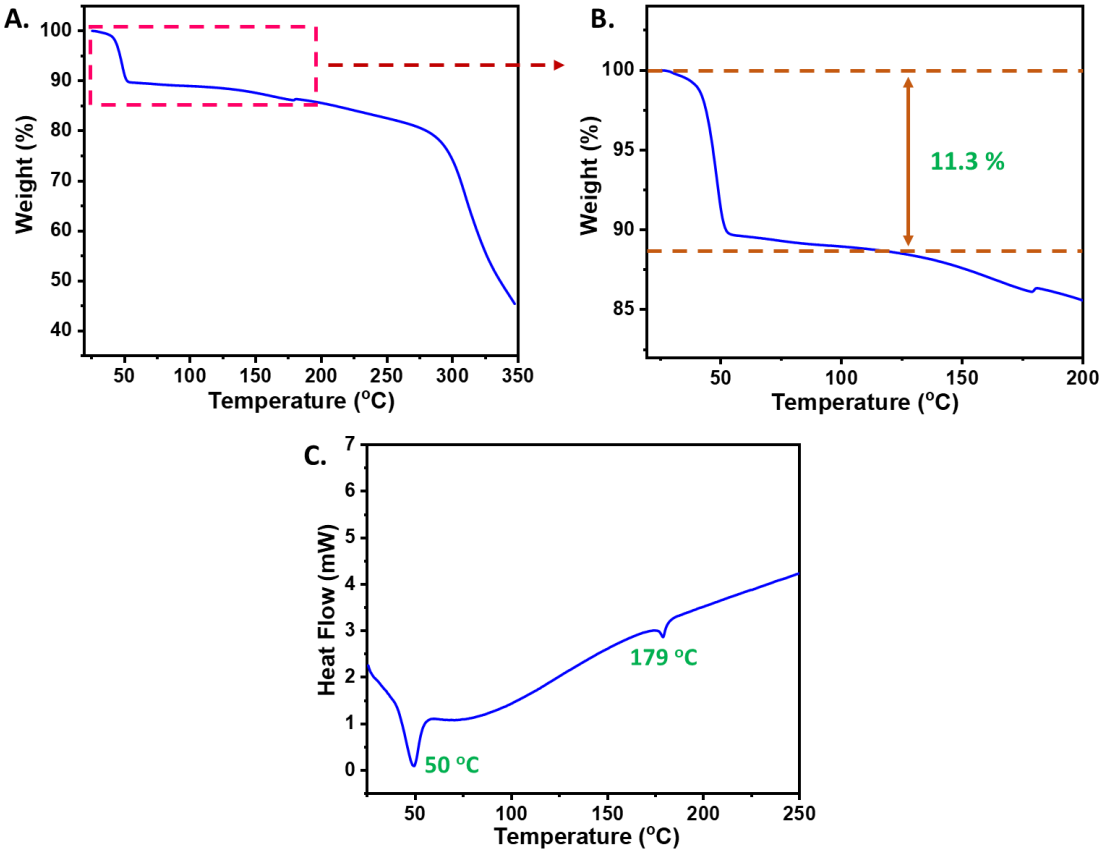

Figure S11. Thermal analysis of the Azo-DPA before crystallization (A) TGA plot showing the decomposition of the sample after 290 °C; (B) Zoomed version of TGA (25 °C to 200 °C) displaying the water loss (11.3%) before 100 °C; (C) DSC data exhibiting water loss around 50 °C, much before melting point (179 °C).

Mechanical properties of the crystal

Nanoindentation experiment:

Determination of hardness (*H*) and modulus (*E*) of the elastic crystal.

Nanoindentation experiments were done using the instrumentation set up from Hysitron Triboindentor, TI Premier, Minneapolis, USA equipped with an in-situ Scanning Probe Microscope (SPM). The instrument measures the force and displacement of the nanoindentation probe with a unique three-plate capacitive transducer design which provides an unsurpassed noise floor (0.2 nm) and ultra-low working force (~ 75 nN). The experiment was done using a Berkovich tip of radius ~ 150 nm. Analysis of the measured load vs. displacement (*P*-*h*) curves (particularly the unloading segment) provides quantitative information on the mechanical properties of the sample. The stiffness, S, was calculated from the slope of the *P*–*h* curve at the very initial point of unloading (i.e., S = dP/dh), therefore *E* and *H* can be found only at the maximum penetration depth. The elastic contact stiffness determined from the *P*–*h* curves is later used to calculate the reduced modulus, E_r, by using the equation $E_r = (\sqrt{\pi}/2\beta)\,(S/\sqrt{A})$, where, A, is the contact area under load (based on the calibrated tip area function) and β is a constant that depends on the geometry of the indenter. The nanohardness, *H*, can be determined from the maximum indentation load, P_{max}, by using the equation, $H = P_{max}/A$, where the contact area (A) is a function of the contact depth, h_c, and can be determined by the following equations, $A = C_0h_c^2 + C_1h_c + C_2h_c^{1/2} + \cdots + C_8h_c^{1/128}$, the constants will be varied with tip geometry. The contact depth, h_c can be determined by the equation $h_c = h_{max} - \varepsilon\,(P_{max}/S)$ where h_{max} is the maximum depth of penetration, where ε is a constant that depends on the geometry of the indenter.

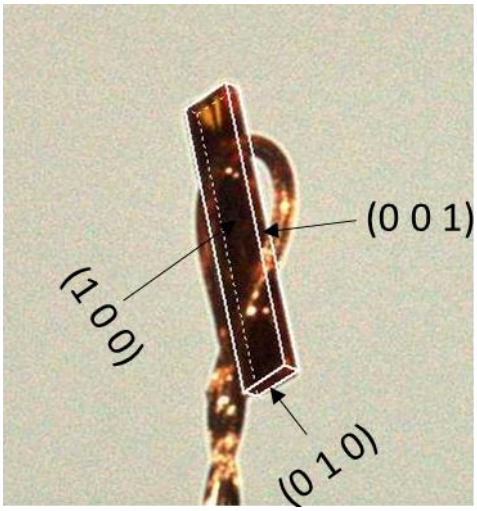

Figure S12: Face indexed image of real crystal.

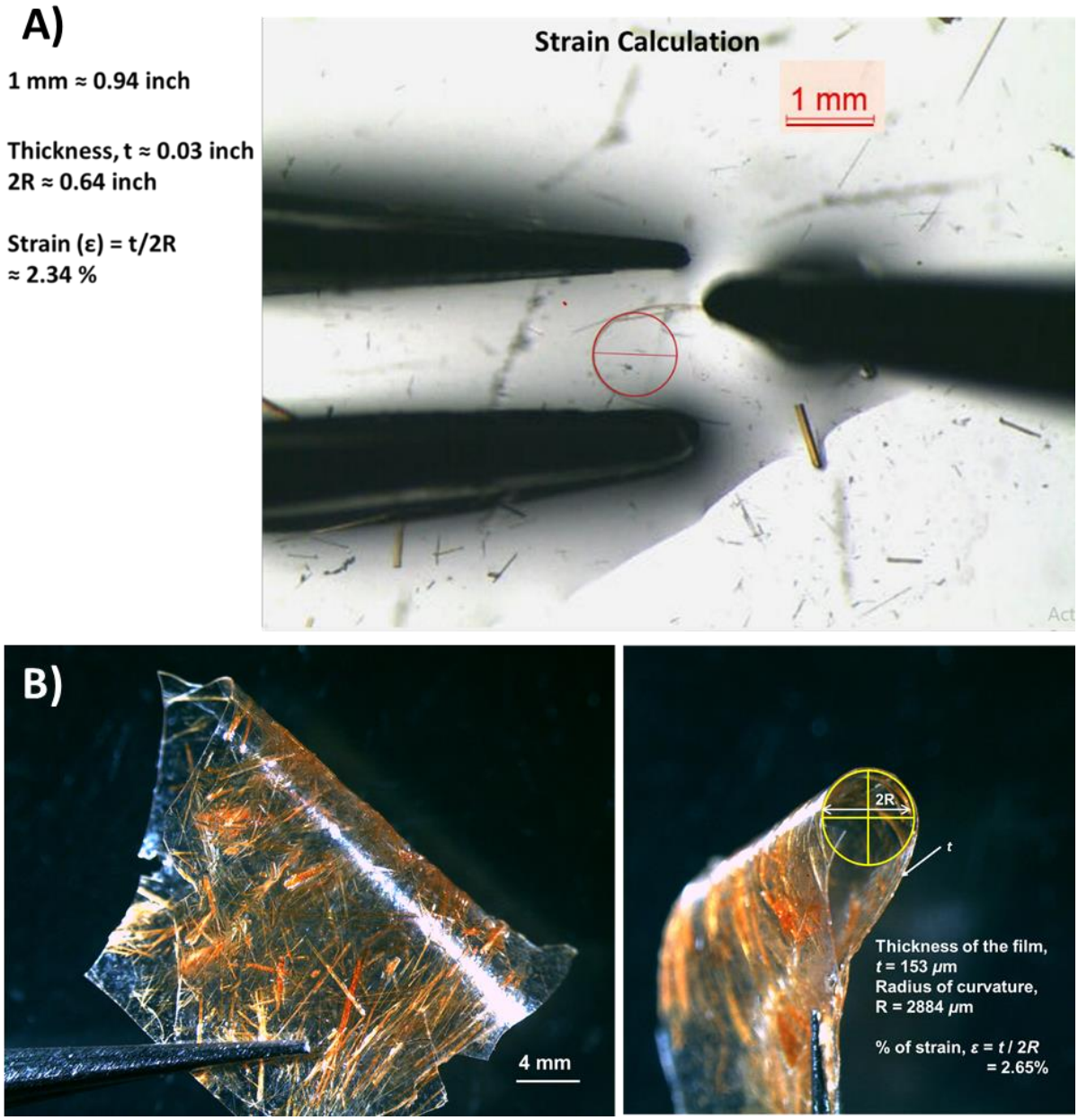

Figure S13: Elastic strain calculation using Euler-Bernoulli's beam bending method **(A)** for single crystal; (B) thin-film using flexible Azo-DPA and PVA (polyvinyl alcohol) polymer.

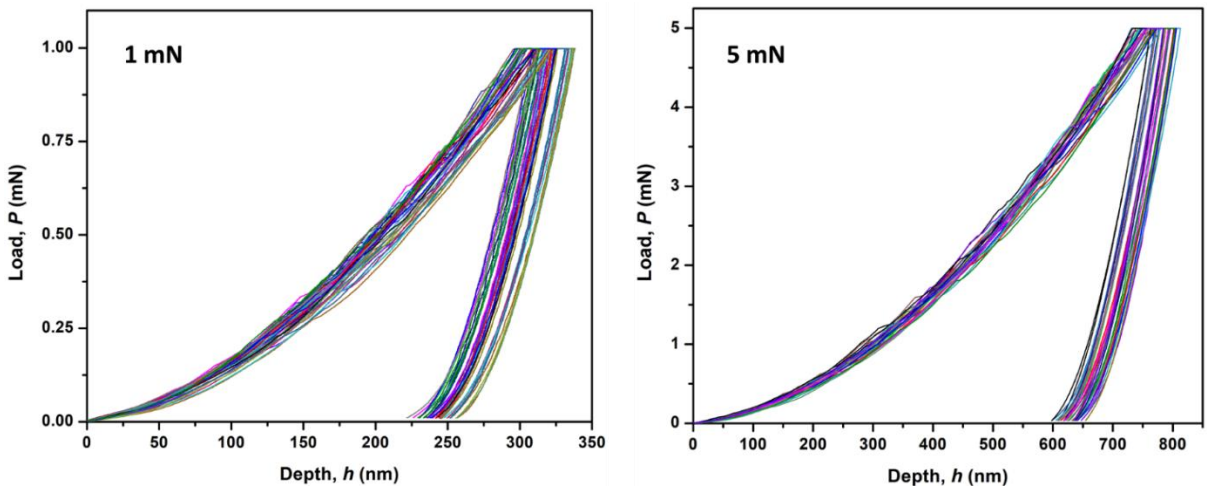

Figure S14: Multiple *P*-*h* curves at different peak loads showing the repeatability of the data.

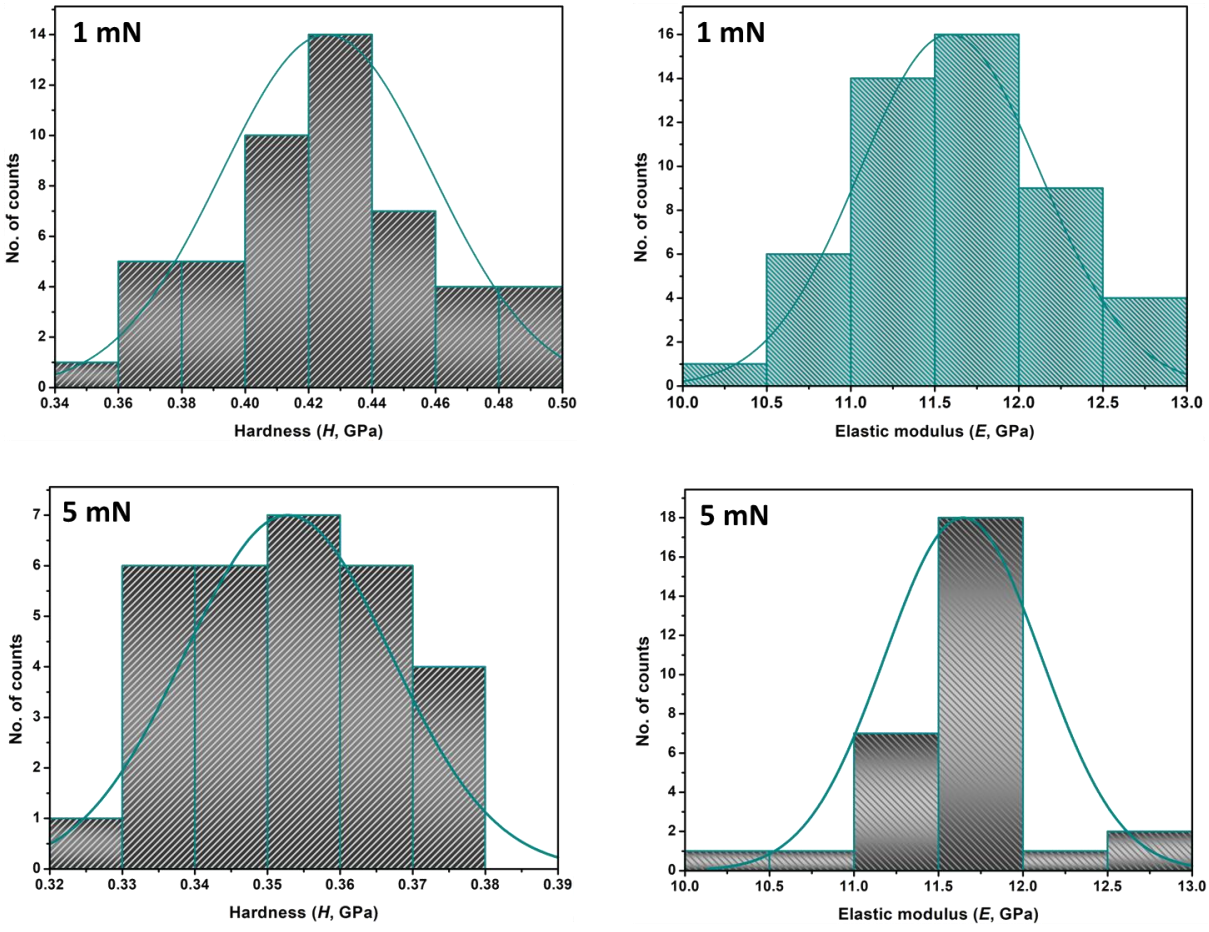

Figure S15: Histogram plots of the data of hardness (*H*) and modulus (*E*) at different loads.

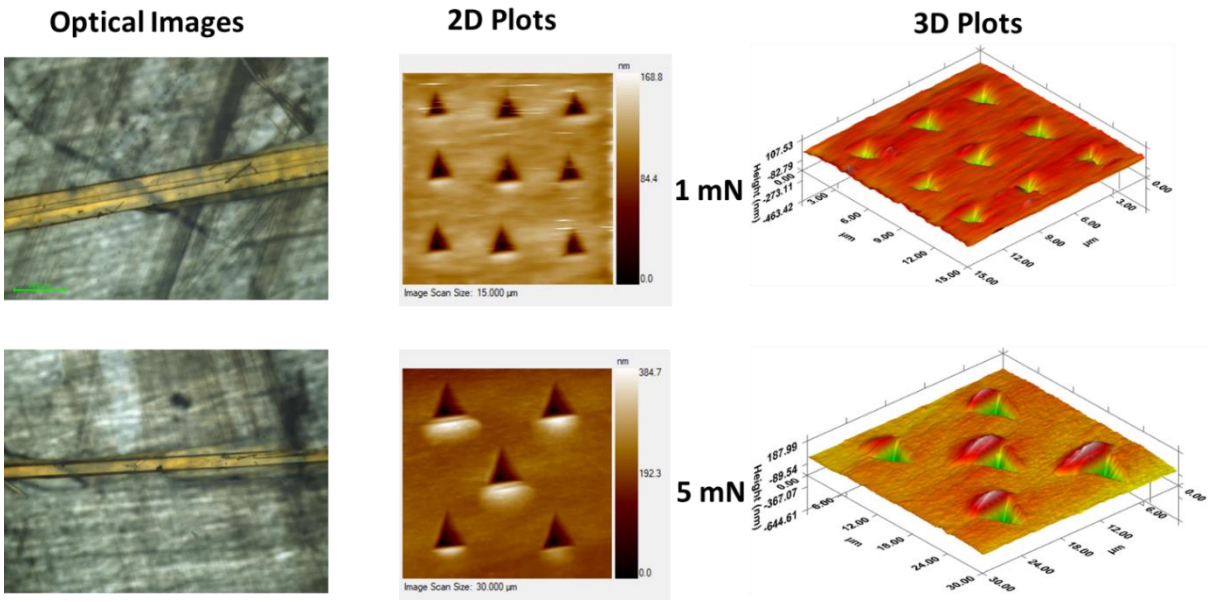

Figure S16: Optical images of the real crystals on which nanoindentation experiments were performed along with multiple 2D & 3D indent impressions at 1mN and 5 mN peak loads.

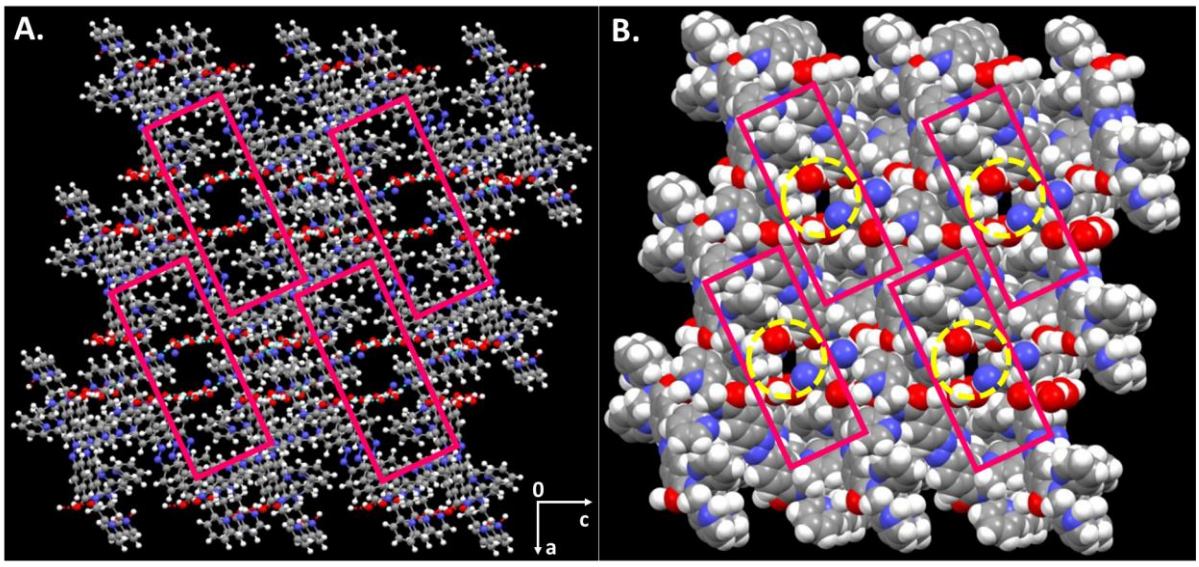

Figure S17: Crystal structure of Azo-DPA (A) Ball and stick and (B) space-filling style. Both the images explicitly display the presence of void space around the water channel. These void spaces actually allow the smooth change in geometry of the water molecules which further allows hydrogen bond reorganization during proton conduction through the water channel.

Electrochemical analysis

Proton conductivity measurement:

The intrinsic proton-conducting property of the Azo-DPA compound before and after crystallization was determined by two-probe A.C impedance measurement using BioLogic VMP-300 instrument. The electrochemical impedance measurements were recorded in the frequency range of 1 MHz-0.1 Hz at a voltage amplitude of 10 mV. Approximately 100 mg of the desired sample was pressed for 1 min into a 13 mm die under 1000 psi to obtain a uniform pellet. The pellet was placed between two stainless-steel electrodes in a homemade setup. A bench top-type environment chamber (SH-222, ESPEC Co. Ltd., Japan) was used to control the temperature and humidity during the impedance measurement accurately. The experiment was carried out at different temperatures (between 10 to 70 ^{o}C at every 10 ^{o}C interval) under 95 % relative humidified conditions. The sample was kept at each temperature for 1 h to reach an equilibrium state before recording the impedance. The ionic conductivity was calculated from the bulk resistance (high-frequency intercept of the Nyquist plot in the impedance data) values at different temperatures using the following equation:

$$\sigma = \frac{L}{R \times A} \ldots \qquad \textbf{Equation S1}$$

Where, σ, L, R, and A represent the conductivity (S cm^{-1}), the thickness of the pellet (cm), bulk resistance (Ω), and area of the pellet (cm^2), respectively.

Table S2: List of proton-conducting material and their proton-conduction value where conduction takes place through the neutral water channel

Sr. No.	Compound name	Conductivity (S.Cm^{-1})	E_a (eV)	Temperature (^{O}C)	Relative humidity (%)	References
1.	As-synthesized Azo-DPA	1.42×10^{-4}	0.30	70	95	*This work*
2.	Crystallized Azo-DPA	4.48×10^{-4}	0.23	70	95	*This work*
3.	Crystallized Azo-DPA	1.63×10^{-4}	0.23	30	95	*This work*
4.	Porous organic cage (CC3)	6.4×10^{-6}	0.11	30	95	*Nat. commun.* **2016**, *7*, 1-9
5.	Cucurbit[6]uril (CB[6] H_2O)	6.6×10^{-6}	0.31 - 0.56	30	95	*Angew. Chem. Int. Ed.* **2011**, *50*, 7870–7873
6.	Pristine HKUST-1 (H_2O-HK)	1.5×10^{-5}	–	25	–	*J. Am. Chem.Soc.* **2012**, *134*, 51–54
7.	PCMOF-3	3.5×10^{-5}	0.17	25	98	*J. Am. Chem. Soc.* **2010**, *132*, 14055–14057
8.	$LaCr(ox)_3 \cdot 10H_2O$	1.0×10^{-5}	0.32	25	95	*Inorg. Chem.* **2015**, *54*, 8529–8535
9.	Mg-NU-225 Fe-NU-225	1.5×10^{-5} 1.7×10^{-5}	0.33 0.42	55	95	*Inorg. Chem.* **2021**, *60*, 1086–1091

Crystallized Azo-DPA displays the highest proton conductivity value amongst the reported neutral organic system (Porous organic cage and Cucurbit [6] uril (CB[6] H_2O)) at 30 ^{O}C. Besides, this system can outclass some of the MOF materials where proton conduction is taking place through the water channel.

Electrochemical evaluation:

At first, the active material Azo-DPA, conducting carbon, and PVDF binder in 80:15:5 weight ratio were thoroughly mixed in 250 µl of NMP to obtain a homogeneous slurry. A required amount of this slurry was coated over a 1.0 cm^2 area of the Grafoil current collector to get a total mass-loading of 1 mg cm^{-2}. Finally, the coated electrodes were dried at 60 ^oC. The electrochemical cells are assembled in CR2032 coin cell using the Azo-DPA electrode as cathode and Zn foil anode separated by a glass fiber separator soaked in desired electrolytes. The aqueous electrolytes are prepared by dissolving 2.5 M $Zn(ClO_4)_2$. $6H_2O$ salt in deionized water or 0.5 M H_2SO_4 solution. The aprotic organic electrolyte contains 0.5 M $Zn(CF_3SO_3)_2$ salt dissolved in acetonitrile solvent. For the electrochemical analysis in three-electrode cell configuration, the electrochemical cell was configured using Azo-DPA coated Grafoil as the working electrode, Pt mesh as the counter electrode, and Hg/Hg_2SO_4 or Ag/AgCl as the standard reference electrode.

Calculation of specific capacity:

Specific capacity (mAh g^{-1}) = $\frac{discharge\ time\ (h) \times applied\ current\ (mA)}{Total\ loading\ of\ electrode\ material\ (mg)} \times 1000$ ..... **Equation S2**

Theoretical capacity (mAh g^{-1})

$= \frac{nF}{3.6 \times MW}$ ..... **Equation S3**

n= 2 (number of electrons involve in redox-reaction); *F*= Faraday constant; *MW*= 632 g/mol (molecular weight of the active material used in the electrode).

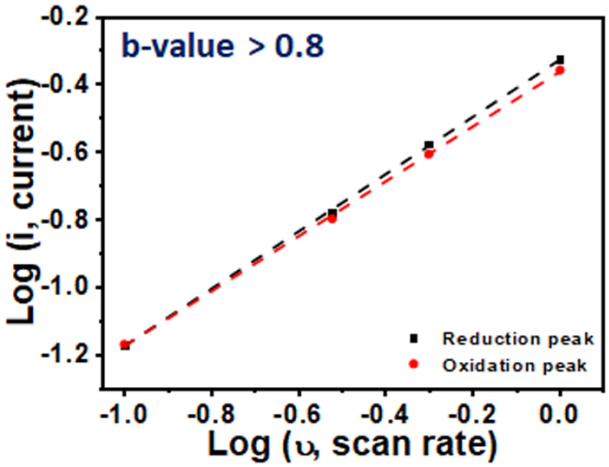

Figure S18: Changes in current response to the scan rates indicating surface-controlled capacitive charge storage process (b-value above 0.8).

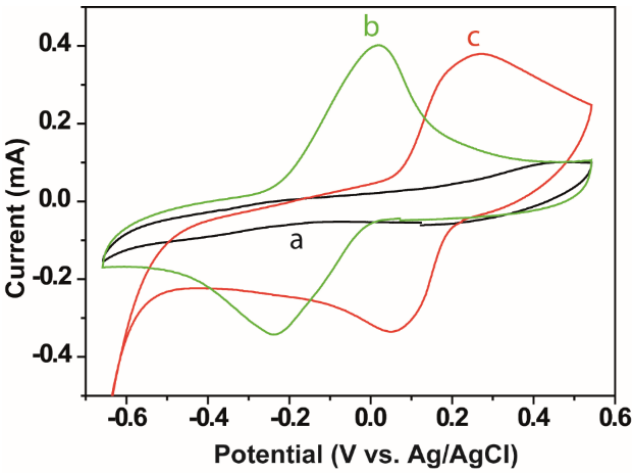

Figure S19: CV profile of the Grafoil current collector (black curve, a) used in this study to prepare the Azo-DPA electrode; CV profiles of Azo-DPA in 1M $Zn(ClO_4)_2/H_2O$ (green curve, b) and 0.1 M $HClO_4/H_2O$ (red curve, c) electrolytes in three-electrode cell configurations at 1 mV sec^{-1} scan rate.

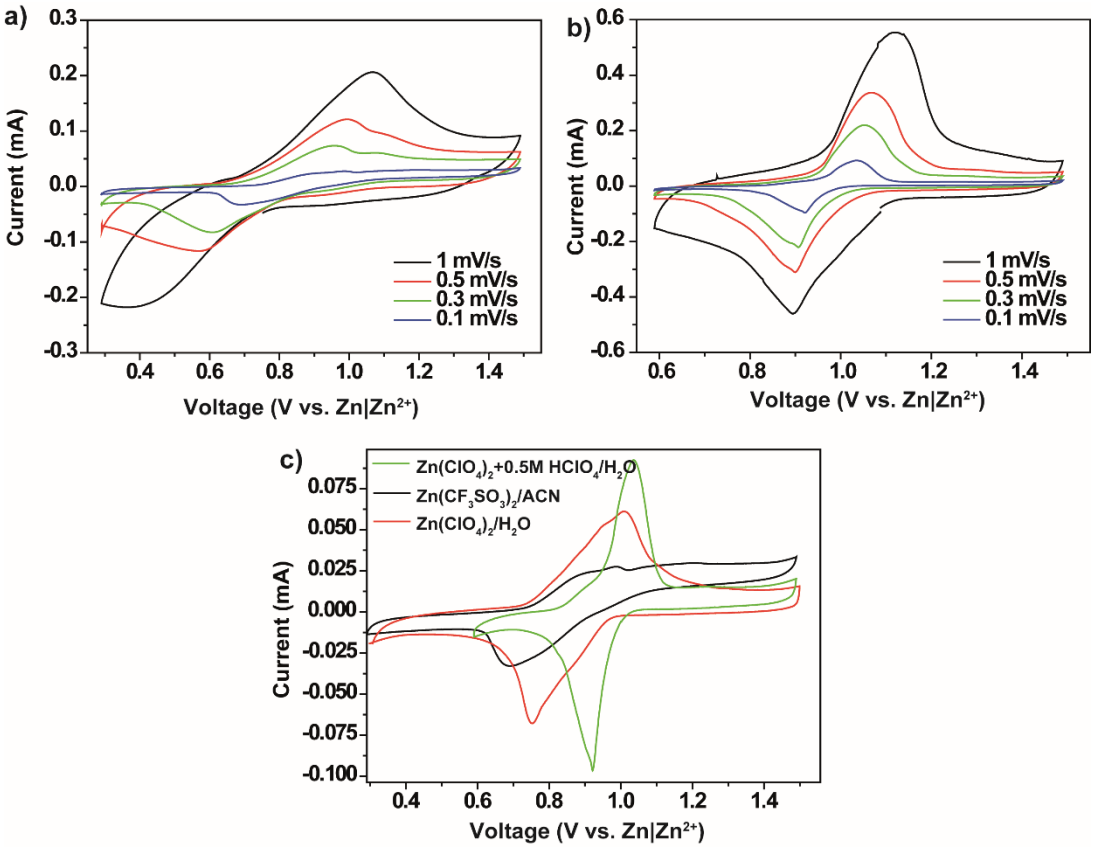

Figure S20. CV profiles at various scan rates for Zn||Azo-DPA cells (two-electrode cell configuration) acquired in (a) 0.5 M $Zn(CF_3SO_3)_2/CH_3CN$ and (b) mixed aqueous electrolytes; (c) comparison of CV profiles for Zn||Azo-DPA cells recorded in various electrolytes at 0.1 mV sec^{-1} scan rate.

Density functional theory (DFT) calculation

The geometry optimization for the electronic ground state was performed using Density Functional Theory (DFT) method using Becke's three-parameter hybrid exchange functional (*5*) combined with Lee-Yang-Parr correlation functional (*6*) abbreviated as B3LYP taking 6-31G as the basis set. All the geometries of Azo-DPA were optimized in a vacuum without any imaginary frequency using Gaussian 09 software package (*7*). 'Gauss View' and 'Avogadro' software was used for the visualization of molecular orbitals. The energy level of HOMO and LUMO of the Azo-DPA molecule were obtained from the optimized geometry. Molecular electrostatic potential (MESP) was obtained from the optimized geometry of Azo-DPA and visualization of the MESP plot was carried out by 'Avogadro software'.

Table S3: Change in azo (N-N) bond distance upon stepwise addition of electrons

Sr. No.	Species	Azo (N-N) bond distance (Å)	Carbonyl (C-O) bond distance (Å)
1.	Azo-DPA	1.27	1.26
2.	1 electron reduction of Azo-DPA	1.34	1.27
3.	2 electron reduction of Azo-DPA	1.39	1.28
4.	Discharge product (H_2Azo-DPA)	1.38	1.26

Upon the addition of electrons to the Azo-DPA, the bond distance of azo (N-N) is found to be increased which implies N=N is the most active redox center in the Azo-DPA system. Although the slight change in the carbonyl bond (C-O) was observed upon the addition of the electron that is simply because of the resonance effect.

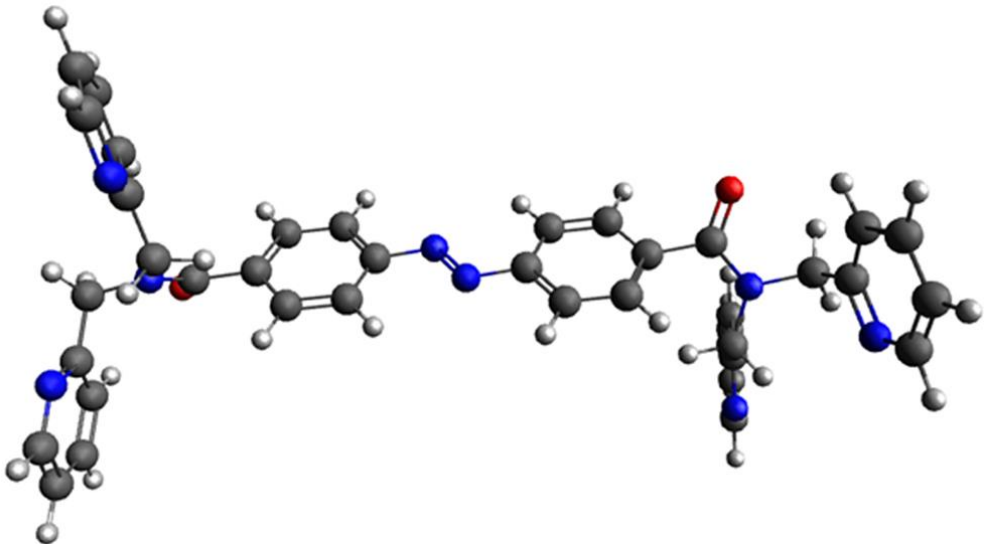

Figure S21. Optimized geometry of Azo-DPA using B3LYP DFT method taking 6-31G as the basis set in a vacuum.

Table S4: Cartesian coordinate of Azo-DPA

0 1

N	0.29677400	-0.04445100	0.28728700
N	-0.40740800	0.05643900	1.34987800
C	-1.80088000	0.26410200	1.14893000
C	1.69006100	-0.25215500	0.48831800
C	-2.57292300	0.36950000	2.31665600
C	-3.94791600	0.57861900	2.23024300
C	-4.57550300	0.65533200	0.97579000
C	-3.79116200	0.56960900	-0.19339000
C	-2.41475600	0.37748300	-0.11185900
C	2.45936400	-0.36213800	-0.67951600
C	3.83865200	-0.55609000	-0.59540200
C	4.46427900	-0.64610100	0.66056700
C	3.67850100	-0.57184800	1.82811000
C	2.30654100	-0.36139600	1.74946700
C	-6.04069300	0.97683400	0.93549000
C	5.92110400	-0.97233800	0.81066700
O	6.25543600	-1.94739000	1.53695900
N	6.86775200	-0.22115900	0.15169600
N	-6.88968700	0.22153300	0.15853100
O	-6.47156600	1.94978300	1.61192100
C	-8.29284100	0.69401800	0.02591300
C	-6.56830400	-1.04887100	-0.50664000
C	8.27407200	-0.69995300	0.20456300
C	6.64277600	1.05116100	-0.54865500
C	8.57921300	-1.64335000	-0.93764500
C	7.10881100	2.27386400	0.22700700
C	-7.12602800	-2.27467700	0.20056300

C	-8.44952700	1.63543700	-1.14751600
N	-8.68460400	1.05687400	-2.35163300
C	-8.80527900	1.85433800	-3.43573100
C	-8.70154000	3.24695000	-3.37019900
C	-8.45178200	3.84024400	-2.12727100
C	-8.32095800	3.02501000	-0.99886700
C	-7.50912100	-2.28370900	1.54839700
C	-7.97411700	-3.47756600	2.11130100
C	-8.03867000	-4.62658700	1.31685200
C	-7.63257600	-4.53337100	-0.01827600
N	-7.18817000	-3.38588000	-0.57191900
N	8.97383900	-1.06720500	-2.10048100
C	9.23304400	-1.86642400	-3.15871700
C	9.11524100	-3.25849100	-3.10670000
C	8.70074900	-3.84925300	-1.90734500
C	8.42570200	-3.03216100	-0.80655300
C	7.30899200	2.28106600	1.61386200
C	7.70154700	3.47242900	2.23429400
C	7.87787400	4.62083600	1.45607800
C	7.65274500	4.52957900	0.07870900
N	7.27955000	3.38449000	-0.52978800
H	-2.07025800	0.29276800	3.27389200
H	-4.54566200	0.69514100	3.12687900
H	-4.26022000	0.68080600	-1.16581400
H	-1.79996100	0.31755900	-1.00121600
H	1.95440500	-0.29704900	-1.63643800
H	4.42348300	-0.66354300	-1.50283000
H	4.16141200	-0.69295200	2.79133600
H	1.69429000	-0.28849700	2.63951200
H	-8.92568400	-0.18113600	-0.13056600
H	-8.56863200	1.18745800	0.95886600

H	-6.96754900	-1.02709600	-1.52550700
H	-5.48540600	-1.15944800	-0.58422400
H	8.92579400	0.17230800	0.13196200
H	8.42295100	-1.19348100	1.16592700
H	7.17239400	1.02784700	-1.50619700
H	5.58004300	1.16717700	-0.76748600
H	-8.99375200	1.35036600	-4.37814700
H	-8.81221200	3.84653900	-4.26698100
H	-8.35975400	4.91778900	-2.03845900
H	-8.10530200	3.43930000	-0.02085200
H	-7.44641100	-1.37743100	2.13937800
H	-8.27931800	-3.50840600	3.15222800
H	-8.39427400	-5.56908400	1.71780000
H	-7.66393900	-5.39710300	-0.67461300
H	9.54668600	-1.36436500	-4.06823700
H	9.34078500	-3.85958700	-3.98065100
H	8.59293500	-4.92627800	-1.83086600
H	8.08096000	-3.44438800	0.13466100
H	7.16300000	1.37537800	2.19087700
H	7.86540800	3.50182700	3.30662600
H	8.18219500	5.56141300	1.90128800
H	7.77615300	5.39295700	-0.56716000

Ground state P.E = –2055.171737 Hartree; Number of imaginary frequencies = 0

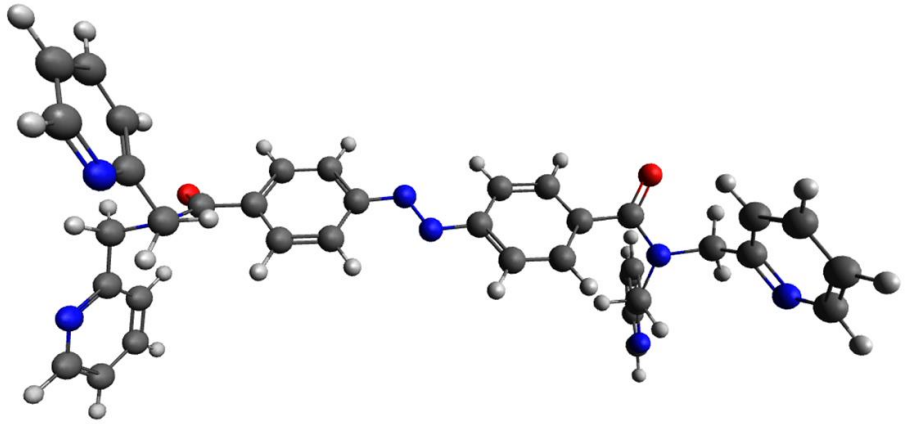

Figure S22. Optimized geometry of Azo-DPA in *trans*-form after 1 electron reduction using B3LYP DFT method taking 6-31G as the basis set in a vacuum.

Table S5: Cartesian coordinate of Azo-DPA after 1 electron reduction

-1 2

N	0.29700400	0.03881000	-0.39453300
N	-0.42616100	-0.04112000	-1.52908800
C	-1.78302900	-0.19311300	-1.33175800
C	1.65352600	0.19273400	-0.59122800
C	-2.60139700	-0.29140900	-2.49245700
C	-3.97262800	-0.44563600	-2.39521200
C	-4.61955100	-0.47803700	-1.13356100
C	-3.80369900	-0.41363000	0.02674500
C	-2.42769300	-0.27903900	-0.06214900
C	2.46787700	0.28522400	0.57168500
C	3.84349700	0.42157100	0.48132800
C	4.49019400	0.48176400	-0.78154500
C	3.67446500	0.44206900	-1.94102000
C	2.30230300	0.28508400	-1.85938500
C	-6.07362600	-0.70463700	-1.10260500
C	5.93487500	0.70460200	-0.95253500
O	6.38553100	1.42111500	-1.89981300

N	6.84725200	0.14359000	-0.04708100
N	-6.85436500	-0.14344800	-0.08215000
O	-6.64768800	-1.42524600	-1.97739700
C	-8.24766300	-0.62845700	0.05242300
C	-6.51342100	1.06351200	0.67897300
C	8.24855200	0.62052500	-0.11181400
C	6.61181600	-1.06322000	0.75323200
C	8.49909700	1.79850400	0.80530000
C	7.22428900	-2.32137500	0.15531900
C	-7.21586000	2.31770000	0.17977000
C	-8.36073800	-1.79806400	1.00685600
N	-9.00454200	-1.57560700	2.17909200
C	-9.10656400	-2.59626800	3.06159400
C	-8.58046500	-3.86690700	2.82247300
C	-7.92051400	-4.09583300	1.60718900
C	-7.80995100	-3.05265100	0.68671600
C	-7.58129100	2.49250800	-1.16446500
C	-8.17310100	3.69656500	-1.55544700
C	-8.38470400	4.69600300	-0.59831700
C	-7.99226300	4.44360700	0.71876200
N	-7.42294000	3.28269300	1.10885600
N	9.28898200	1.58012600	1.88543900
C	9.51809100	2.60870600	2.73423600
C	8.97993400	3.88356500	2.55074700
C	8.16809000	4.10803200	1.43030400
C	7.92510900	3.05662300	0.54526400
C	7.39056100	-2.49479400	-1.22789400
C	7.90981500	-3.70229900	-1.70244900

C	8.24919500	-4.70625500	-0.78775400
C	8.05299500	-4.45489900	0.57262700
N	7.55524800	-3.29083500	1.04309000
H	-2.10479600	-0.24642900	-3.45625600
H	-4.58268000	-0.54373600	-3.28736100
H	-4.25985700	-0.52559100	1.00721100
H	-1.80340100	-0.24946900	0.82184300
H	1.96659700	0.25824500	1.53372600
H	4.42603600	0.53837100	1.39096900
H	4.15985800	0.53600800	-2.90781500
H	1.68315600	0.23413400	-2.74590100
H	-8.86965000	0.18312200	0.43358500
H	-8.59103000	-0.91884000	-0.94407800
H	-6.76556700	0.93228500	1.73633100
H	-5.43634900	1.22943800	0.61977000
H	8.91228100	-0.19184600	0.18864400
H	8.45318100	0.89891900	-1.14906000
H	7.01699500	-0.93602400	1.76241500
H	5.53639900	-1.22108400	0.85199800
H	-9.62879600	-2.37213100	3.98709300
H	-8.68426700	-4.65269200	3.56342600
H	-7.50031600	-5.07115500	1.38233700
H	-7.31143600	-3.18212600	-0.26741500
H	-7.40393200	1.69741500	-1.87921700
H	-8.46153400	3.85298900	-2.59021100
H	-8.84106500	5.64355800	-0.86409800
H	-8.13705800	5.18666200	1.49738500
H	10.15521800	2.38770600	3.58557700

H	9.19001200	4.67592900	3.26159900
H	7.73333400	5.08635300	1.25063000
H	7.30611200	3.18171000	-0.33613300
H	7.11829000	-1.69646100	-1.90833800
H	8.04426600	-3.85787100	-2.76830400
H	8.65456200	-5.65655000	-1.11846100
H	8.30261700	-5.20150900	1.32072900

Ground state P.E = –2055.231036 Hartree; Number of imaginary frequencies = 0

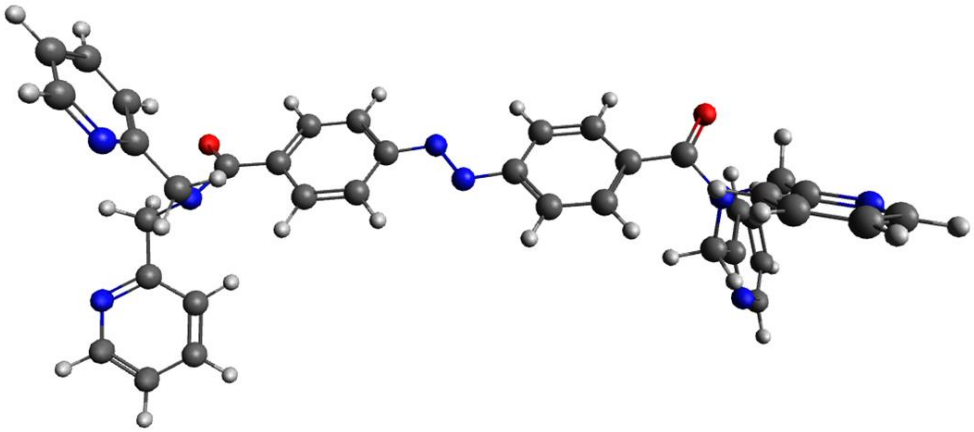

Figure S23. Optimized geometry of Azo-DPA in *trans*-form after 2 electron reductions using B3LYP DFT method taking 6-31G as the basis set in a vacuum.

Table S6: Cartesian coordinate of Azo-DPA after 2 electron reductions

-2 1			
N	0.29675300	0.02661600	-0.60233000
N	-0.46535100	-0.05062800	-1.76517400
C	-1.78850100	-0.16182800	-1.56311600
C	1.61994200	0.13850300	-0.80278400
C	-2.64763900	-0.25185800	-2.72328100
C	-4.00872400	-0.36982500	-2.61662000
C	-4.67437500	-0.39707000	-1.34098800
C	-3.82188300	-0.32907100	-0.18387800
C	-2.45611200	-0.21979800	-0.27859900
C	2.46980700	0.23409300	0.36175900
C	3.83506100	0.34252800	0.26606500
C	4.50738100	0.37214800	-1.00684800
C	3.66071900	0.30682200	-2.16800900
C	2.29719100	0.18939500	-2.08415100
C	-6.09176600	-0.54023800	-1.29514100
C	5.91650000	0.50592700	-1.17307000
O	6.50607300	0.80544000	-2.27703700

N	6.76965800	0.29591500	-0.01002400
N	-6.77027100	-0.29575800	-0.02965200
O	-6.83103500	-0.87672800	-2.29362700
C	-8.03309900	-1.00360400	0.18230800
C	-6.64226500	1.00623700	0.62937600
C	8.05410100	0.99681000	-0.00749500
C	6.73267400	-0.98451500	0.70080600
C	8.18987800	1.99093700	1.12740800
C	7.54042200	-2.09927700	0.04555600
C	-7.54926300	2.09461300	0.06561100
C	-7.99433900	-1.95670100	1.35937900
N	-9.17925600	-2.22531600	1.96988300
C	-9.18767100	-3.09457200	3.00553900
C	-8.04136100	-3.73374200	3.48110400
C	-6.82028300	-3.45744200	2.84839300
C	-6.79550100	-2.55989200	1.77993100
C	-8.06548300	2.03691300	-1.24248400
C	-8.86011200	3.09212900	-1.69915000
C	-9.12265600	4.17564400	-0.85035200
C	-8.57342500	4.15424200	0.43328000
N	-7.80514300	3.14168400	0.89192700
N	9.45050800	2.26037800	1.56017100
C	9.61149400	3.16526400	2.55201600
C	8.54931200	3.84088700	3.15520400
C	7.24964400	3.56387800	2.70550200
C	7.06753100	2.62947400	1.68504600
C	7.86065800	-2.08738700	-1.32484800
C	8.57324000	-3.16484700	-1.85846200

C	8.94979300	-4.22471100	-1.02266000
C	8.59376500	-4.15797200	0.32581700
N	7.90707100	-3.12345600	0.85904700
H	-2.15709100	-0.22348700	-3.69272100
H	-4.63132500	-0.44352100	-3.50378200
H	-4.27560400	-0.40907300	0.80238800
H	-1.82691300	-0.19077300	0.60264400
H	1.97091900	0.23330100	1.32736300
H	4.42303800	0.45224500	1.17455500
H	4.15133600	0.34991200	-3.13711600
H	1.67639900	0.13192100	-2.96982700
H	-8.87962300	-0.31977800	0.32990000
H	-8.23739500	-1.55210700	-0.74777900
H	-6.85334100	0.91435400	1.70225500
H	-5.60421300	1.34160500	0.54021300
H	8.90900200	0.30944000	0.04199000
H	8.12509400	1.50987100	-0.97687400
H	7.09961500	-0.86226600	1.72779400
H	5.69067300	-1.31152500	0.77531600
H	-10.15628900	-3.27368800	3.46659600
H	-8.10082700	-4.42145000	4.31914700
H	-5.90335100	-3.93273200	3.18422400
H	-5.87719500	-2.30519400	1.26483800
H	-7.84747700	1.17690300	-1.87046700
H	-9.26593600	3.06954000	-2.70647500
H	-9.73511100	5.01208200	-1.17341800
H	-8.75031300	4.97031800	1.12975600
H	10.63629800	3.34347700	2.86965200

H	8.73164300	4.55689700	3.95077100
H	6.39352600	4.06755400	3.14476800
H	6.08431400	2.37248900	1.30983200
H	7.55873000	-1.24493600	-1.94175900
H	8.82742400	-3.17780800	-2.91441000
H	9.50294700	-5.07745400	-1.40466500
H	8.86502100	-4.95440900	1.01468800

Ground state P.E = –2055.184077 Hartree; Number of imaginary frequencies = 0

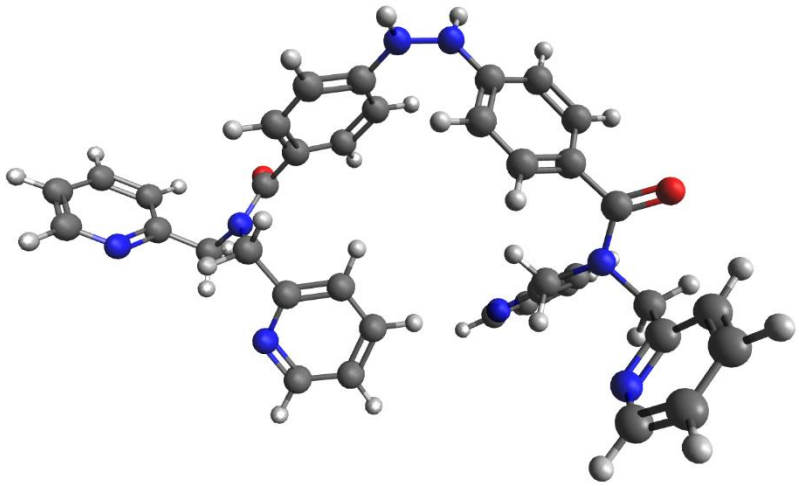

Figure S24. Optimized geometry of the discharge product **H_2Azo-DPA** using B3LYP DFT method taking 6-31G as the basis set in a vacuum.

Table S7: Cartesian coordinate of the discharge product (H_2Azo-DPA)

0 1			
N	-0.53207700	-4.78554500	0.15292100
N	0.60798300	-4.51386200	0.88313000
C	1.55308800	-3.56152500	0.47521700
C	-1.62587200	-3.91494600	0.11381700
C	2.55465000	-3.15345000	1.37764200
C	3.47938500	-2.17820900	1.00721400
C	3.43910600	-1.59191200	-0.27054700
C	2.47283900	-2.04748500	-1.18183300
C	1.52780300	-3.00455100	-0.81653100
C	-1.70668400	-2.79818900	0.96579000
C	-2.78862800	-1.92432000	0.87087300
C	-3.81580200	-2.13432300	-0.06517400
C	-3.75904000	-3.28935400	-0.86606100
C	-2.67725700	-4.16080100	-0.79333700
C	4.45027700	-0.59067300	-0.73702400
C	-5.02020800	-1.25751300	-0.16405500
O	-6.17237700	-1.76987700	-0.19150400
N	-4.86181900	0.11674100	-0.22409300

N	4.67008400	0.54457300	0.01039500
O	5.09224600	-0.79998200	-1.80270300
C	5.76264600	1.45302300	-0.42496000
C	3.78908500	1.05626700	1.08816900
C	-6.08685800	0.95222200	-0.13239300
C	-3.60999700	0.83712700	-0.48782700
C	-6.35000600	1.38784500	1.29137500
C	-3.40013300	1.21516200	-1.94623600
C	2.80315800	2.09589800	0.58592000
C	7.09185700	1.03232800	0.16224600
N	7.36495900	1.47906300	1.41431000
C	8.53210900	1.11337100	1.98763500
C	9.47195600	0.29812300	1.34983000
C	9.18380700	-0.16894900	0.06230200
C	7.97704100	0.19944800	-0.54000400
C	1.53503300	1.73916800	0.10104600
C	0.67009700	2.73607400	-0.36381800
C	1.10581800	4.06702500	-0.33321800
C	2.38528200	4.34403500	0.15555500
N	3.22277700	3.38548800	0.61018700
N	-5.74408500	2.53358000	1.69171000
C	-5.92496600	2.94532300	2.96632200
C	-6.70946800	2.24521000	3.88725700
C	-7.32788800	1.05951600	3.47291500
C	-7.14490200	0.62164300	2.15801700
C	-4.23430700	0.79126600	-2.98834500
C	-3.93658300	1.18421900	-4.29821900
C	-2.81329900	1.98262100	-4.53351800
C	-2.02577700	2.35619700	-3.44050000
N	-2.30783100	1.98678000	-2.17304200
H	-0.48034100	-5.54533900	-0.51014600

H	0.62868700	-4.84931500	1.83562800
H	2.60392700	-3.59863100	2.36784900
H	4.24844400	-1.88045800	1.71331300
H	2.46636500	-1.63872600	-2.18641200
H	0.77089200	-3.32096300	-1.52352800
H	-0.92238900	-2.61635100	1.68982500
H	-2.84243300	-1.08255800	1.55400900
H	-4.57514900	-3.49210200	-1.55074500
H	-2.63991700	-5.03463200	-1.43807000
H	5.80165100	1.43787200	-1.51565700
H	5.50989900	2.45602200	-0.07804500
H	3.25153500	0.22293400	1.53675300
H	4.43215600	1.51119800	1.84509900
H	-5.94191600	1.83760500	-0.75482300
H	-6.91836200	0.36129800	-0.51829100
H	-3.60470000	1.74946800	0.11881500
H	-2.75473100	0.24016200	-0.17304400
H	8.71048000	1.49473800	2.98826400
H	10.39901400	0.03720000	1.84874700
H	9.88506300	-0.80996800	-0.46233500
H	7.69899700	-0.16108500	-1.52319600
H	1.23513000	0.69637300	0.08589900
H	-0.31718500	2.48373600	-0.74452700
H	0.46604400	4.87185900	-0.67875300
H	2.76307300	5.36080100	0.19453800
H	-5.42345300	3.86671200	3.24418300
H	-6.83074700	2.61865600	4.89808100
H	-7.94115000	0.48715800	4.16125400
H	-7.58981500	-0.29966200	1.79931500
H	-5.09255400	0.16506700	-2.77650900
H	-4.57097300	0.86871100	-5.12009100

H	-2.55021000	2.30520700	-5.53442900
H	-1.13839500	2.96669700	-3.57117800

Ground state P.E = –2056.402399 Hartree; Number of imaginary frequencies = 0

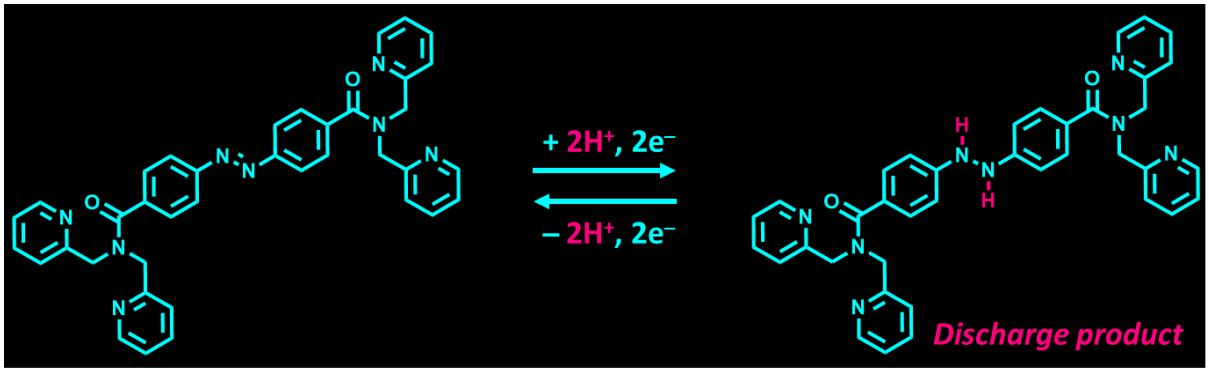

Figure S25. Coordination reaction between Azo-DPA and carrier (H^+) during the discharge process.

The binding energy of the coordination reaction between Azo-DPA and carrier (H^+).

Ground state potential energy of Azo-DPA = –2055.1717 Hartree;

Ground state potential energy of 2H = –1.0005 Hartree;

Ground state potential energy of discharge product (H_2Azo-DPA) = –2056.4023 Hartree

Binding energy = [(–2056.4023) – {(–2055.1717) + (–1.0005)}] Hartree = − 0.2301 Hartree

The binding energy of the coordination reaction between Azo-DPA and H^+ is − 0.2301 Hartree (− 6.261 eV) which facilitates the formation of the discharge product but Zn^{2+} cannot form a similar discharge product with the single Azo-DPA as Zn^{2+} prefer tetrahedral geometry (geometrical constrain). These results suggest the insertion of H^+ over Zn^{2+} in the Zn/Azo-DPA system.

References

(1) Dolomanov, O. V.; Bourhis, L. J.; Gildea, R. J.; Howard, J. A. K.; Puschmann, H. OLEX2: A Complete Structure Solution, Refinement and Analysis Program. *J. Appl. Cryst.* **2009**, *42*, 339–341.

(2) G. M. Sheldrick, SHELXT—Integrated space-group and crystal-structure determination. *Acta Crystallogr. A* **2015**, *71*, 3–8.

(3) Sheldrick, G. M. A Short History of SHELX. *Acta Crystallogr. A* **2008**, *64*, 112–122.

(4) S. Ghosh, D. Usharani, A. Paul, S. De, E. D. Jemmis and S. Bhattacharya, *Bioconjugate Chem.* **2008**, *19*, 2332-2345.

(5) A. D. Becke, *Phys. Rev. A.* **1988**, *38*, 3098–3100.

(6) C. Lee, W. Yang. R. G. Parr, *Phys. Rev. B.* **1988**, *37*, 785–789.

(7) Frisch, M. J.; Trucks, G. W.; Schlegel, H. B.; Scuseria, G. E.; Robb, M. A.; Cheeseman, J. R.; Scalmani, G.; Barone, V.; Mennucci, B.; Petersson, G. A.; Nakatsuji, H.; Caricato, M.; Li, X.; Hratchian, H. P.; Izmaylov, A. F.; Bloino, J.; Zheng, G.; Sonnenberg, J. L.; Hada, M.; Ehara, M.; Toyota, K.; Fukuda, R.; Hasegawa, J.; Ishida, M.; Nakajima, T.; Honda, Y.; Kitao, O.; Nakai, H.; Vreven, T.; Montgomery, J. A.; Jr., Peralta, J. E.; Ogliaro, F.; Bearpark, M.; Heyd, J. J.; Brothers, E.; Kudin, K. N.; Staroverov, V. N.; Kobayashi, R.; Normand, J.; Raghavachari, K.; Rendell, A.; Burant, J. C.; Iyengar, S. S.; Tomasi, J.; Cossi, M.; Rega, N.; Millam, J. M.; Klene, M.; Knox, J. E.; Cross, J. B.; Bakken, V.; Adamo, C.; Jaramillo, J.; Gomperts, R.; Stratmann, R. E.; Yazyev, O.; Austin, A. J.; Cammi, R.; Pomelli, C.; Ochterski, J. W.; Martin, R. L.; Morokuma, K.; Zakrzewski, V. G.; Voth, G. A.; Salvador, P.; Dannenberg, J. J.; Dapprich, S.; Daniels, A. D.; Farkas, O.; Foresman, J. B.; Ortiz, J. V.; Cioslowski, J.; Fox, D. J. Gaussian 09, Revision A.1. Gaussian, Inc.; Wallingford CT: **2009**.